Czech Technical University in Prague
Faculty of Electrical Engineering
Department of Cybernetics

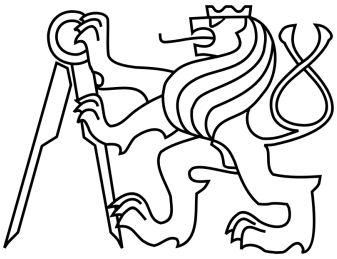

BACHELOR THESIS

RRT-path method used for cooperative surveillance by group of helicopters

Author: Matěj Račinský

Thesis supervisor: Dr. Martin Saska

In Prague, 2016

Název práce: Aplikace algoritmu RRT-path v úloze autonomního dohledu skupinou helikoptér

Autor: Matěj Račinský

Katedra (ústav): Katedra kybernetiky

Vedoucí bakalářské práce: Dr. Martin Saska

e-mail vedoucího: saska@labe.felk.cvut.cz

Abstrakt V předložené práci studujeme... Uvede se abstrakt v rozsahu 80 až 200 slov. Lorem ipsum dolor sit amet, consectetuer adipiscing elit. Ut sit amet sem. Mauris nec turpis ac sem mollis pretium. Suspendisse neque massa, suscipit id, dictum in, porta at, quam. Nunc suscipit, pede vel elementum pretium, nisl urna sodales velit, sit amet auctor elit quam id tellus. Nullam sollicitudin.

Klíčová slova: klíčová slova (3 až 5)

Title: RRT-path method used for cooperative surveillance by group of helicopters

Author: Matěj Račinský

Department: Department of Cybernetics

Supervisor: Dr. Martin Saska

Supervisor's e-mail address: saska@labe.felk.cvut.cz

Abstract In the present work we study ... Uvede se anglický abstrakt v rozsahu 80 až 200 slov. Lorem ipsum dolor sit amet, consectetuer adipiscing elit. Ut sit amet sem. Mauris nec turpis ac sem mollis pretium. Suspendisse neque massa, suscipit id, dictum in, porta at, quam. Nunc suscipit, pede vel elementum pretium, nisl urna sodales velit, sit amet auctor elit quam id tellus. Nullam sollicitudin. Donec hendrerit. Aliquam ac nibh. Vivamus mi. Sed felis. Proin pretium elit in neque. Pellentesque at turpis. Maecenas convallis. Vestibulum id lectus.

Keywords: klíčová slova (3 až 5) v angličtině

Prohlašuji, že jsem svou bakalářskou práci napsal(a) samostatně a výhradně s použitím citovaných pramenů. Souhlasím se zapůjčováním práce a jejím zveřejňováním.

V Praze dne 5th May 2016 Jméno Příjmení + podpis

CONTENTS

CHAPTER
ONE

INTRODUCTION

Unmanned Aerial Vehicle, abbreviated as UAV is an aircraft intended to operate with no pilot on-board. The UAV is also known as drone and it has been gaining popularity in recent years in both academic circles and wide public. The term Micro Aerial Vehicle (MAV) is also used sometimes. In recent news in the media, combat drones, used during conflicts in the Middle East, were mentioned quite often. But the drones are used mainly for peaceful purposes. For small drones, the quadrotor (also called quadcopter) design has become very popular and widely used. Quadrotor is a multirotor helicopter that is lifted and propelled by four horizontal rotors. Quadrotors are used in the Multi-Robot Systems group at CTU, which assembles their own quadrotors. Example of this quadrotor can be seen in figure.

Figure 1.1: DYI quadrotor assembled in the Multi-Robot Systems group at CTU

CHAPTER
TWO

ALGORITHM

The basis of the whole algorithm is shown in 2.1 in the pseudocode.

The configuration variable is instance of the Configuration class, which holds all configuration data, including a selected map. The map holds all Areas of Interest (AoI) and obstacles. All obstacles and AoIs are represented as rectangles now.

The purpose of the path finding is to find the shortest feasible paths, but real UAVs need to have some minimal distance to obstacles due to weather conditions, sensor errors and other aspects. To solve this issue, every obstacle is amplified before the whole path finding algorithm on line 2. This minimal distance to obstacles allows UAVs to follow their trajectories safely.

The 3rd line represents the discretization of the map to the graph. The discretization divides the map to squares with size set in the configuration and each square is represented by a graph node. In this graph, there are 4 types of nodes: Free, Obstacle, UAV and Goal. If the whole square or its part is covered by an obstacle, the corresponding node has the type Obstacle. If the whole square or its part is covered by an AoI, then the corresponding node has type Goal. If the square contains an UAV, the corresponding node has type UAV and rest of squares have corresponding nodes with type Free.

Edges in this graph are only between nodes of neighbouring squares, so each node has maximally 8 edges. Obstacle nodes do not have any edges.

After converting the map to nodes, the optional grouping of goals for guiding path can be

Algorithm 2.1 The basis of whole algorithm

```
1:  map := configuration.getMap();
2:  map := amplifyObstacles(map);
3:  nodes := mapToNodes(map);
4:  paths := createGuidingPaths(nodes);
5:  rrtPath := rrtPath(paths, map, nodes);
6:  lastState := getBestFitness(rrtPath, map);
7:  path := getPath(lastState);
8:  path = straightenCrossingTrajectories(path);
9:  path := resamplePath(path, map);
10: path := optimizePathByDubins(path, map);
11: savePath(path);
```

enabled. I will cover the grouping in chapter 4.

The 4th line represents the calculation of the guiding paths for RRT-Path algorithm using the A* algorithm with modified cost function. The modification will be covered in section 3.3.

On the 5th line the RRT-Path algorithm takes place. This function returns a structure with a tree with a root at the starting position of UAVs and with an array containing leaves of this three, where all UAVs are in Areas of Interest.

The leaf, where UAVs have the best coverage of AoI, is chosen on the 6th line. The quality of the coverage is determined by the cost function, which is described in chapter 5.

On the 7th line the path is built from the last state.

On the 8th line there is an optional preparation before the optimization using Dubins curves. In the preparation, all crossings of paths of individual UAVs are straightened, so UAVs do not cross other trajectories during the whole path. Details are covered in the chapter6.

On the 9th line, the re-sampling of the path is made, mainly due to requirements of real UAVs, which are mentioned in chapter 9.

On the 10th line there is the optimization by Dubins curves. The optimization is covered in chapter 8.

The last line represents persisting of the path to a file for usage of path by different programs. Path is persisted to JSON, due to convenience of the JSON format. JSON is smaller than XML and can be easily parsed by all widely used programming languages. Path is also persisted to CSV format, so it can be loaded to MATLAB and then loaded into real UAVs.

CHAPTER
THREE

RRT-PATH

This chapter will cover brief introduction of RRT-Path algorithm. In first of all, we need to define RRT algorithm which RRT-Path is based on.

3.1 Rapidly Exploring Random Tree

Rapidly Exploring Random Tree, also abbreviated as RRT, introduced by LaValle[3] in 1998, is non-deterministic algorithm for motion planning, used to search non-convex spaces by randomly building space-filling tree. The RRT method builds a tree T rooted at q_{start}. The basic RRT algorithm works as follows. In each iteration, a random sample q_{rand} is chosen from C and the nearest node q_{near} in the tree to q_{rand} is found. The node q_{near} is expanded using a local planner to obtain a set of new configurations reachable from q_{near}. The nearest configuration towards q_{rand} is selected from this set and added to the tree. The edge from q near rand to the newly added configuration contains control inputs used by the local planner to reach the new configuration. The algorithm terminates if the distance between a node in the tree and q_{goal} is less than d_{goal} or after I_{max} of planning iterations. [7] The basis of RRT is listed in algorithm 3.1. In RRT algorithm, configurations on the third line have uniform distribution.

3.2 RRT-Path

RRT-Path, introduced by Vonásek [7] in 2015, is an improved version of RRT featuring preprocessing of configuration space. RRT-Path enables UAVs to manoeuvre around obstacles and find way in narrow passages. RRT. Path also finds goal much faster [5]. RRT-Path uses the guiding path during building the space-filling tree. Before running RRT algorithm, the guiding path from q_{start} to q_{goal} is found and sampled. One of inputs to RRT-Path algorithm is the probability $p\,(guided)$. In the main loop of the algorithm, obtaining of the random configuration is modified. Instead of random configuration with uniform distribution, configuration around the $q_i$is selected with probability $p\,(guided)$.

Let G be the guiding path and $\left(q_{start}, q_1, q_2, ..., q_{goal}\right) \in G$ the points of the guiding path, where $q_i \in C_{free}$. In the beginning, $q_i = q_1$, so random point is selected from area around the point q_1 with probability $p\,(guided)$. When the leaves of the searching tree reach distance lower than $r_{dist}$to the q_i, then the next point of the guiding path will be used instead of q_i, so $q_i := q_{i+1}$. This continues until q_{goal} is reached, which means the RRT-Path algorithm ends.

Algorithm 3.1 RRT algorithm source [7]

Input: Configurations q_{alert} and q_{goal}, maximum number of iterations I_{max}, maximum distance to goal d_{goal}

Output: Trajectory P or failure

```
1:  T.add (q_start) ; // create new tree and add initial conguration q in it
2:  for iteration:=1:I do
3:     q_rand := getRandomConfiguration(C);
4:     q_near := nearest node in tree T to q ;
5:     expandTree(q_rand,q_near);
6:     d = distance from tree T to q_goal ;
7:     if d < d then
8:        P = extract trajectory from q_start to q_rand;
9:        return P;
10:    end
11: end
12: return failure; // no solution was found within K iterations start
```

3.3 Guiding path

The guiding path is obtained by transferring the map to graph representation and then path is found using the graph-search algorithms. The map can be transferred to graph representation by using the Voronoi diagram, visibility graph or by discretization to a grid representation.

Then the path can be found by using Dijkstra algorithm or A* algorithm. In this thesis, the A* algorithm has been used because of its ability to find optimal path and easy calculation of heuristic function is Euclidean space.

The classic cost function of node q_i in A* algorithm is $f(q_i) = g(q_i) + h(q_i)$. The $g(q_i)$ is sum of costs of all edges in shortest path between nodes and q_{init} and q_i. The $h(q_i)$ is heuristic estimate of distance between q_i and q_{goal}. In Euclidean space, it is calculated as $h(q_i) = \left\| q_i - q_{goal} \right\|$. This algorithm uses a modified cost function and in addition to a cost function of the A* algorithm. The modified cost function is $f(q_i) = g(q_i) + h(q_i) + j(q_i)$, where $j(q_i)$ is number representing the nearness to the nearest obstacle. For example, it can be $j(q_i) = \frac{const}{\|q_i - nearest\,obstacle\|}$, where $const$ is weight of the $j(q_i)$ and expresses how much obstacles should be avoided with respect to length of the whole path.

CHAPTER
FOUR

GROUPING OF GOALS FOR THE GUIDING PATH

During this processing of the map (method MapProcessor::getEndNodes in codebase) all AoIs are grouped to one big AoI, which is the smallest rectangle covering all AoIs.

If this modification is enabled, only one goal is used for all AoIs instead of one goal for every AoI (node in the middle of AoI rectangle is considered to be the goal node). The whole swarm has only one guiding path, so the grouping prevents swarm from splitting. The relative localization is the main reason to have only one big swarm instead of more smaller swarms (or individual UAVs in case of the same count of AoI and UAVs). Advantages of relative localization are more significant when we have only one big swarm.

Grouping of goals is done by finding the smallest rectangle containing all AoIs. Middle of this big rectangle is considered to be middle of the group of goals. When obstacle is in the middle, nearest node which is not obstacle is used as middle of goals group. The middle is used as target for guiding path.

This approach has the following advantage: when individual AoIs are near to a global goal of the whole group, as seen in 4.2, then the whole swarm follows one guiding path without any splitting, which makes the RRT-Path run faster and also the advantage of relative localization is included.

Maps with goals and obstacles are shown in figures 4.1 and 4.2. Goals are coloured green colour and obstacles grey.

The disadvantage of this method appears when individual AoIs have a bigger distance from each other than can be covered by UAVs. Then this approach totally fails, because RRT-Path, which is much faster than RRT, has goal very distant from AoIs, as can be seen in 4.1 and main part of the path is found by RRT algorithm, which is slower.

Because of advantages of having only one swarm, all experiments in this thesis use grouping and all UAVs form one big swarm.

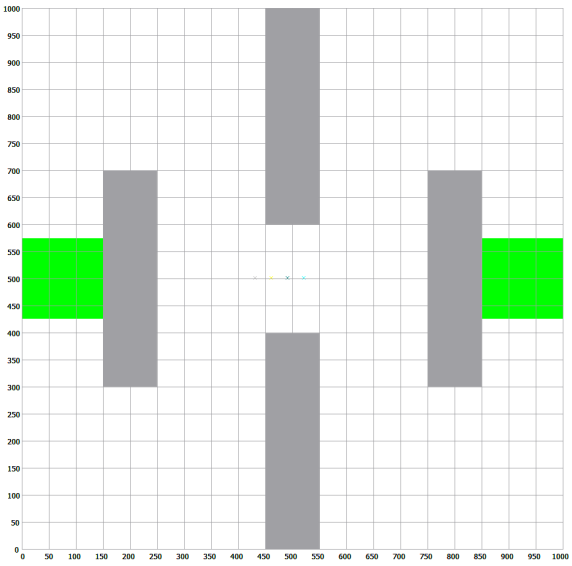

Figure 4.1: Map with goals unsuitable for grouping

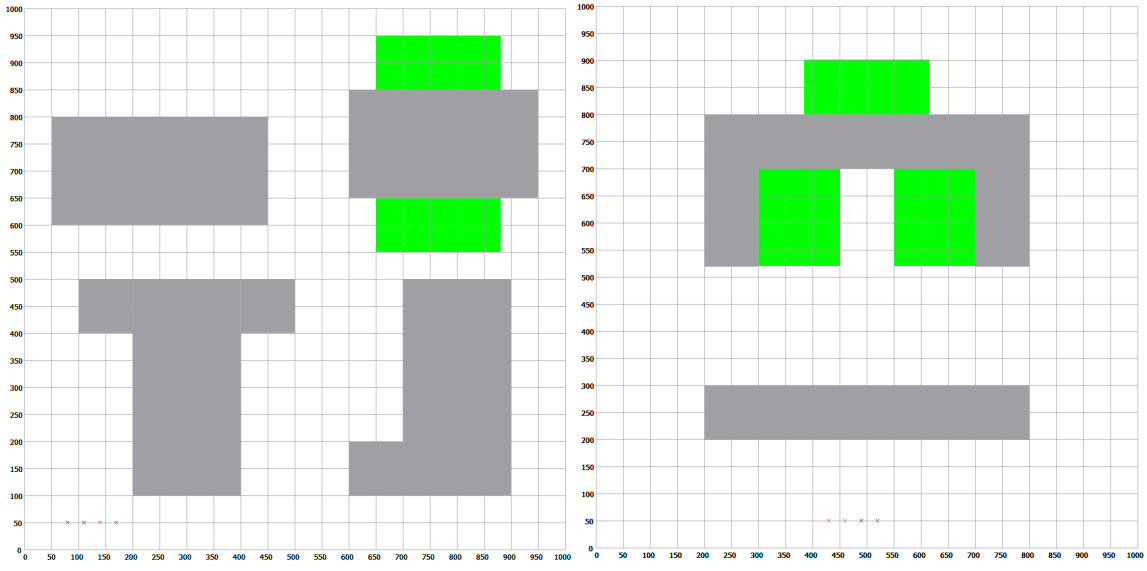

Figure 4.2: Maps with goals suitable for grouping

CHAPTER
FIVE

AREAS OF INTEREST COVERAGE

Covering Areas of Interest (AoIs) with UAVs is key part of task of autonomous or cooperative surveillance. In task of surveillance, UAVs view space below them by on-board camera, as shown in figure 5.1. AoIs and areas seen by UAVs are represented by rectangles in this thesis for simplicity and fast computation.

Coverage of AoIs is optimization problem. This optimization problem can be solved by finding minimum of cost function. The value of cost function should objectively reflect the quality of coverage, the lower value should represent better coverage. In this thesis, cost function $f\ (q_i)$ represents quality of coverage in configuration q_i, where configuration q_i is set of UAV positions. The cost function f in this thesis measures size of AoIs not covered by UAVs, which is equivalent to information not seen by UAVs. That means if $f\ (q_1) < f\ (q_2)$ configuration q_1 covers bigger part of AoIs than configuration q_2. The world $W = R^2$ is discretized to square grid represented by matrix $A \in R^2$. One of parameters for coverage optimization is size of one square in grid $a\ [map]\ units$. Element $A_{j,k}$ represents square with size a and left lower corner with coordinates $[j \cdot a, k \cdot a]$. Before computing areas seen by UAVs, $A_{j,k}$=A_{max} if it contains AoI, and $A_{j,k} = 0$ otherwise. $A_{max} = 100$ has been used in experiments, but the value is arbitrary. Then the

$$A_{j,k} := A_{j,k} \cdot l^m$$

formula is applied to every element of the world representing matrix A. Variable l must be in

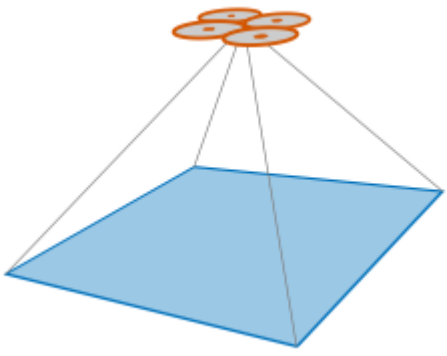

Figure 5.1: The area viewed by UAV on-board camera, source [5]

0	0	0	0	0	0	0	0	100	100	100	100	100	100	100	100	100	0	0	0
0	0	0	0	0	0	0	0	100	100	100	100	100	100	100	100	100	0	0	0
0	0	0	0	0	0	0	0	50	50	50	50	50	50	100	100	100	0	0	0
0	0	0	0	0	0	0	0	50	50	50	50	50	50	100	100	100	0	0	0
0	0	0	0	0	0	0	0	50	50	50	50	50	50	100	100	100	0	0	0
0	0	0	0	0	0	0	0	50	50	50	50	50	50	100	100	100	0	0	0
0	0	0	0	0	0	0	0	0	0	0	0	0	0	0	0	0	0	0	0
0	0	0	0	0	0	0	0	0	0	0	0	0	0	0	0	0	0	0	0
0	0	0	0	0	0	0	0	0	0	0	0	0	0	0	0	0	0	0	0
0	0	0	0	0	0	0	0	0	0	0	0	0	0	0	0	0	0	0	0

Figure 5.2: AoI matrix with one UAV, source [5]

range $1 > l > 0$ and represents amount of information not seen by UAV even if this UAV covers the element $A_{j,k}$. This is because quality of image obtained from on-board camera depends on many factors, such as time of day, weather conditions, flight altitude, camera chip resolution, lens parameters, stabilization, frame rate and so on. In this implementation, $l = 0.5$, but if the flight altitude will be considered in the optimization algorithm, higher flight altitude would lead worse image recording, so $l(flightAltitude_1) > l(flightAltitude_2)$ for $flightAltitude_1 > flightAltitude_2$. Variable $m \in N_0$ represents number of UAVs seeing the area of element $A_{j,k}$. Example can be seen in figure 5.2. AoI is marked with green colour and UAV is marked with blue colour. As we can see, parts of AoI not seen by an UAV have value $A_{j,k} = A_{max} = 100$ and parts of AoI seen by UAV have value $A_{j,k} = A_{max} \cdot l^m = 100 \cdot 0.5^1 = 50$.

When UAV arrives above any AoI, RRT-Path algorithm ends for this UAV and instead of it, RRT algorithm takes place. Random node for RRT algorithm is selected only from AoI beneath the UAV, not from whole world. When all UAVs arrive to their goal by RRT-Path algorithm, RRT algorithm is run and it runs until being stopped. After stopping, all states found by RRT algorithm where UAVs are above AoIs, are gathered and their coverage cost function is calculated. State with lowest cost function is used as result of the path finding algorithm and used as input for Dubins curves optimization.

CHAPTER
SIX

PATHS STRAIGHTENING

In the RRT-Path algorithm, crossing paths between neighbouring states are checked, so no trajectories are crossing each other between the n-th state and the $n+1$-th state, but this does not solve the problem completely. In figure 6.1 trajectories found by RRT-Path algorithm are shown. Every colour marks one state in RRT-Path. As we can see, check in algorithm prevents from crossing path between neighbouring states, but crossing of paths in different times can not be easily prevented. We can see in image, that paths cross between points J (yellow), M (light green) and H (orange), K (yellow), so there is no easy approach to prevent path collisions between $n-2$-th state and n-th state. Optimization by Dubins curves shortens trajectory of UAVs, so UAVs could be in these trajectories in different time. Considering that, there could be collisions after optimization. Another complication occurs, when time difference between two states is too low, then UAVs could collide, because in reality UAV can not follow path precisely, but only with some errors.

todo: větší písmena u obrázku

There were attempts to straighten crossing trajectories, but all of them failed. Straightening was done by switching parts of crossing paths from the earliest crossing state to the end. But then lengths of paths differed, which was unsuitable for path planning for swarm. This can be done by adding "waiting" points, points in different state but with the same position in different time. Due to these facts, it was really complicated to straighten longer path with many crossings (this path is really short, paths in other maps are much longer and more complicated). Motion model with inertia is unable to stop immediately in one place, so path waiting states is hard to follow precisely. This fact complicates following the straightened trajectories. Due to all complications mentioned above, this part was removed from algorithm. But it is possible to add it, when better approach will be found.

Figure 6.1: Crossing paths

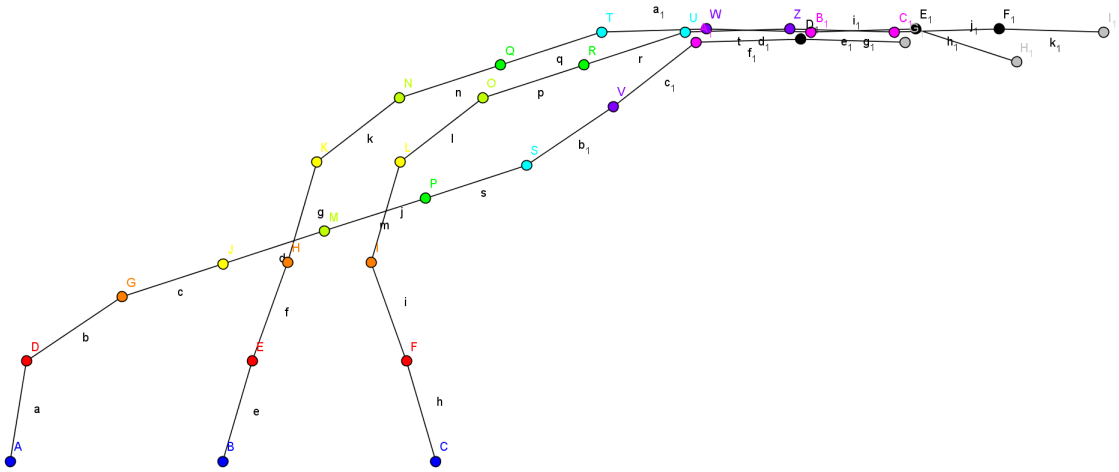

CHAPTER
SEVEN

UAV SWARM PROPERTIES

7.1 Motion model

The RRT-Path algorithm is universal and works with any motion model, which is fine for holonomic robot, but usage of non-holonomic motion model allows us to find path more feasible for swarm of UAVs. For this purpose, car like model was chosen. Car like model is very fast to compute and can be computed analytically. Differential equations of motion model in 3D from [**?**] are

$$\begin{aligned} \dot{x}(t) &= v(t)\sin\varphi(t) \\ \dot{y}(t) &= v(t)\cos(t) \\ \dot{z}(t) &= w(t) \\ \dot{\varphi}(t) &= K(t)\,v(t) \end{aligned} \tag{7.1}$$

where $x(t), y(t), z(t)$ are coordinates of UAV, $\varphi(t)$ represents heading of UAV, $v(t)$ is forward velocity, $K(t)$ is curvature, $w(t)$ is ascent velocity. Vector $\begin{bmatrix} K(t) & w(t) & v(t) \end{bmatrix}$ represent the input vector of motion model. Differential equations are readable and useful for representation in equations, but not they are so useful for computer algorithm due to time consumption. Difference equations are better for usage in algorithm instead of differential equations because they are much faster and scalable. When inputs are held constant in each time interval between two time steps, difference equations are

$$\begin{aligned} x(k+1) &= \begin{cases} x(k) + \frac{1}{K(k+1)}\left(\sin\left(\varphi(k) + K(k+1)\,v(k+1)\,\Delta t(k+1)\right) - \sin(\varphi(k))\right) \\ if\ K(k+1) \neq 0 \\ x(k) + v(k+1)\cos(\varphi(k))\,\Delta t(k+1) \\ if\ K(k+1) = 0 \end{cases} \\ y(k+1) &= \begin{cases} y(k) - \frac{1}{K(k+1)}\left(\cos\left(\varphi(k) + K(k+1)\,v(k+1)\,\Delta t(k+1)\right) - \cos(\varphi(k))\right) \\ if\ K(k+1) \neq 0 \\ y(k) + v(k+1)\sin(\varphi(k))\,\Delta t(k+1) \\ if\ K(k+1) = 0 \end{cases} \\ z(k+1) &= z(k) + w(k+1)\,\Delta t(k+1) \\ \varphi(k+1) &= \varphi(k) + K(k+1)\,v(k+1)\,\Delta t(k+1) \end{aligned} \tag{7.2}$$

7.2 Relative localization

When swarm consists of only one UAV, no relative localization is needed. But when more UAVS are in swarm, every UAV has to be aware of its neighbours in order to remain together in one swarm. In this thesis, relative localization is implemented by setting the minimal distance d_{min} and maximal distance d_{max}. The minimal distance is set because UAV push air beneath them when they fly. UAVs in the Multi-Robot Systems group at CTU have weight around 3 kg, which means 3 kg of air needs to be pushed below UAV in order to keep it flying. Because of this, UAVs can not fly too close to each other because of air currents they produce. The minimal distance is minimal distance in which UAVs do not affect each other by air currents. In last measurements, the minimal distance was 2 meters. The maximal distance needs to be set because of sensors range. UAVs in the Multi-Robot Systems group at CTU use on-board camera based localization system, published in [2]. Sensors have maximal range and UAVs in bigger distance than this maximal range can not be seen. In experiments, the maximal distance was 5 meters.

In configuration of whole algorithm, number of neighbours n is set. Every UAV must have n or more neighbours in distance d, where $d_{min} < d < d_{max}$ in every step of configuration. Default setting is $n = 2$. Computation of this relative localization is fast, but unusable for more than 5 UAVs. Swarm of 6 or more UAVs can split to 2 or more groups and still fit this relative localization constraint. The only solution to check whether all UAVs are in same swarm can be obtained by using following algorithm, which consists of two steps and uses graph representation. Every UAV is node and every pair of UAVs with distance d, where $d_{min} < d < d_{max}$ are connected by an edge. If the graph has only one connected component, all UAVs are in one swarm. Otherwise, the graph has more connected components, which implies UAVs are split into more swarms.

In the first step, the adjacency matrix A is built. Each UAV represents one column and one row in this matrix. The adjacency matrix A is built by following pattern.

$$A_{i,j} = \begin{cases} 1 & if\ d_{min} < d_{i,j} < d_{max} \\ 0 & otherwise \end{cases}$$

where i, j are indices of matrix A and $d_{i,j}$is distance between i-th and j-th UAV. In the second step, the graph represented by A is traversed by depth-first algorithm, starting at $A_{1,1}$. When all nodes are visited during the traversing, the graph has only one connected component and all UAVs are in one swarm. In configuration can be set whether swarm splitting is enabled or not.

CHAPTER

EIGHT

DUBINS CURVES

Dubins curves, also called Dubins manoeuvrers or Dubins path were published by Lester Eli Dubins in 1957 [1]. Dubins path is optimal path for car like motion model. Path is optimal, when car moves at constant forward speed. The other important constraint is the maximum steering angle ϕ_{max}, which results in a minimum turning radiusρ_{min}. As the car travels, consider the length of the curve in $\mathcal{W} = \mathbb{R}^2$ traced out by a pencil attached to the centre of the car. The task is to minimize the length of this curve as the car travels between any q_I and q_G. Due to ρ_{min}, this can be considered as a bounded-curvature shortest-path problem. If $\rho_{min} = 0$, then there is no curvature bound, and the shortest path follows a straight line in $\mathbb{R}^2$. In terms of a cost function, the criterion to optimize is

$$L(\tilde{q}, \tilde{u}) = \int_0^{t_F} \sqrt{\dot{x}(t)^2 + \dot{y}(t)^2} dt \tag{8.1}$$

, where t_F is the time at which q_G is reached, and a configuration is denoted as $q = (x, y, \theta)$, $\tilde{x}_t$ denotes the function $\tilde{x}_t : [0, t] \rightarrow X$, which is called the state trajectory (or state history). This is a continuous-time version of the state history, which was defined previously for problems that have discrete stages. Similarly, $\tilde{u}_t$ denotes the action trajectory (or action history),. If q_G is not reached, then it is assumed that $L(\tilde{q}, \tilde{u}) = \infty$. [4]

When considering constraints of inputs (actions) for motion model, the system can be simplified to

$$\begin{aligned} \dot{x} &= \cos\theta \\ \dot{y} &= \sin\theta \\ \dot{\theta} &= u \end{aligned} \tag{8.2}$$

in which u is chosen from the interval $U = \{-\tan\phi_{max}, 0, \tan\phi_{max}\}$. For simplicity, assume that $\tan\phi = 1$. The following results also hold for any $\phi_{max} \in (0, \pi/2)$.

It was shown in [1] that between any two configurations, the shortest path for the Dubins car can always be expressed as a combination of no more than three motion primitives. Each motion primitive applies a constant action over an interval of time. Furthermore, the only actions that are needed to traverse the shortest paths are $u \in \{-1, 0, 1\}$. The primitives and their associated symbols are shown in 8.1. The S primitive drives the car straight ahead. The L and R primitives turn as sharply as possible to the left and right, respectively. Using these symbols, each possible kind of shortest path can be designated as a sequence of three symbols that corresponds to the

Table 8.1: The three motion primitives from which all optimal curves for the Dubins car can be constructed.

Symbol	Steering u
L	-1
S	0
R	1

order in which the primitives are applied. Let such a sequence be called a word . There is no need to have two consecutive primitives of the same kind because they can be merged into one. Under this observation, ten possible words of length three are possible. Dubins showed that only these six words are possibly optimal:

$$\{LRL,\ RLR,\ LSL,\ LSR,\ RSL,\ RSR\}. \tag{8.3}$$

The shortest path between any two configurations can always be characterized by one of these words. These are called the Dubins curves.

8.1 Optimization using Dubins curves

Because of the fact that Dubins curves provide us optimal trajectory, they can be used to optimize trajectory found with RRT-Path algorithm.

For only one UAV, the situation is quite simple and optimization works as follows.

Two random points of trajectory are chosen and Dubins curves are calculated between them. If calculated curves do not collide with the obstacles, they are used instead of original trajectory between chosen points. This points choosing and trajectory replacing is repeated until the whole trajectory can not be shortened more and thus is optimal.

In real situation, we do not know whether found trajectory is optimal or not, so we need to determine conditions for stopping the optimization. The optimization is stopped if the trajectory is not shortened after many (e. g. 150) iterations or optimization is too slow and path is shortened only by small distances (e. g. shortening by 5% per 1000 iterations).

But in swarm, the situation is complicated because of relative localization and minimal and maximal distances between individual UAVs.

So the algorithm must be modified. Dubins curves must be sampled in same frequency as rest of trajectory (this is frequency of RRT-Path algorithm or higher frequency when path is being re-sampled) and each point has to be validated for feasibility in terms of minimal and maximal distance from another UAVs. So the curves can be used only when all trajectories between minimal and maximal distance of relative localization.

Due to using random points during optimization, the optimization is stochastic and non-deterministic.

8.1.1 One UAV demonstration

In 8.1 we have trajectory of one UAV found by RRT-Path algorithm in map with one obstacle marked by dark grey rectangle. Obstacle amplification is marked by light grey rectangle. In 8.2 we can see optimal path found using Dubins curves. The resulting path consists of many Dubins

Figure 8.1: One UAV before Dubins curves optimization

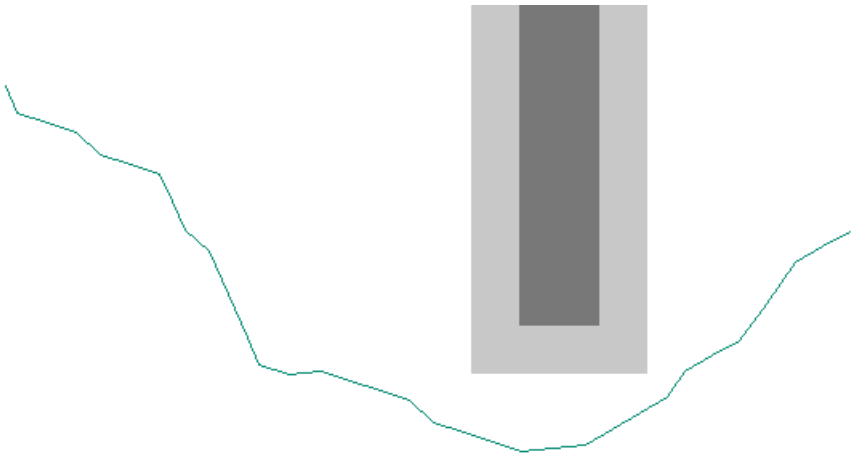

Figure 8.2: One UAV after Dubins curves optimization

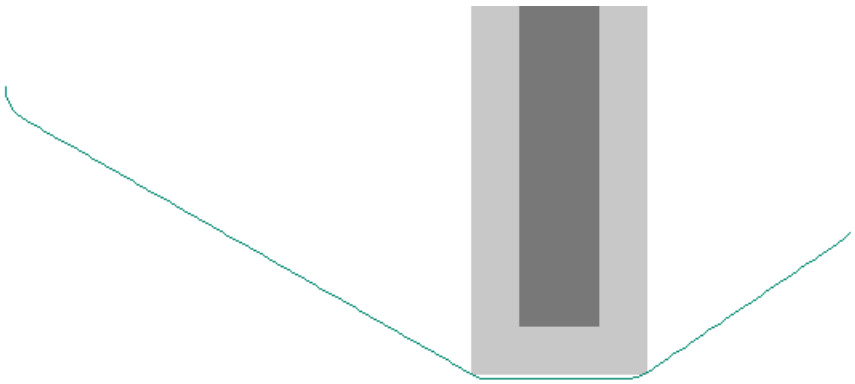

curves and it was obtained by algorithm mentioned above. Random points have been replaced by Dubins curves and after many iterations, optimal path was found.

CHAPTER
NINE

PATH RE-SAMPLING

Motion model in RRT-Path algorithm uses constant input in range from 0.5 to 1 second. Smaller interval for constant input causes RRT-Path algorithm to run for too long. When using too short constant input interval, the tree has too many nodes, grows slowly and runs out of memory much faster than longer interval. Interval longer than 1 second makes UAVs unable to manoeuvre between smaller obstacles. Thus range from 0.5 to 1 second was experimentally chosen as best interval. Using x seconds long constant input interval also means $\frac{1}{x}Hz$ frequency of points in resulting trajectory in output of the algorithm. So the range from 0.5 to 1 second implies resulting frequency is in range 1Hz to 2Hz.

Real UAVs in Multi-Robot Systems group at CTU use frequency 70Hz for providing target points to UAVs and trajectories with lower frequency are linear interpolated to have frequency 70Hz. That means frequency 2Hz is too low for real usage because trajectory generated with this frequency would not be smooth enough.

Change of frequency before the RRT-Path algorithm makes the algorithm unable to run efficiently in bigger maps, so this approach does not solve the problem.

Another solution is to re-sample the path after Dubins curves. But this method failed because after Dubins optimization, the curves had different length and different constant input durations.

The best solution for this problem is re-sampling of trajectory generated by RRT-Path algorithm before it is optimized by Dubins curves. This solution also has big advantage in Dubins curves optimization because it results to shorter final path as will be shown in following experiment.

CHAPTER
TEN

COVERING MORE AOIS WITH ONE SWARM

Some maps have distribution of obstacles and AoIs where algorithm stated above fails. These maps can be seen in figure 10.1. Standard algorithm which uses only one guiding path always leads swarm to only one Area of Interest and the second area remains completely uncovered.

In case of using relative localization where every UAV needs only 1 to 2 neighbours, UAVs can create chain and reach to more distant targets or targets divided by obstacles which UAVs can not reach when moving as one swarm using standard RRT-Path algorithm.

Following modifications must be done if we want to cover all AoIs in figure 10.1.

UAVs are split to two groups, and every group has its own guiding path to one AoI. Relative localization keeps all UAVs in one swarm by its constraints described in section 7.2. With this setting, the swarm behaves like chain, because it is "pulled" to opposite sides by different guiding paths, but it is also connected by relative localization, so it does not split into more smaller swarms. Successful coverage by using the chain behaviour can be seen in figure 10.2.

Unfortunately, this approach does not work in all maps and configurations as can be seen in figure 10.3. The map on the right shows typical example of getting stuck in local minimum, where all UAVs preferred covering only one AoI over covering both AoIs, but the map on the left shows different issue. When we have symmetric map and UAVs do not have starting position in middle of this map, one side of the chain needs to be "pulled" with more power than the other side to cover both AoIs and encircle the obstacle between UAVs starting position and AoIs. This leads to configuration where only one side of chain covers AoI and the other side of chain does not reach the second AoI. This bigger pulling power, which would probably solve this issue, can not be simulated in RRT-Path algorithm. These problems demonstrates the fact this approach is not robust and needs manual preprocessing of UAVs starting positions. The limitation of this approach is also the fact it works only for two AoIs.

10.1 Proposition of improvement of the algorithm

This approach could be modified to be more robust and usable in more maps with more than 2 AoIs. Generalization of this approach would require not crating a chain, which is good only for covering two AoIs, but tree structure, where each leaf covers one AoI. I will now propose principle of the generalized algorithm.

In the first step, we need to decide, which AoIs can be covered by swarm. Some maps can have distant AoIs where all AoIs could not be covered at the same time. This requires finding shortest

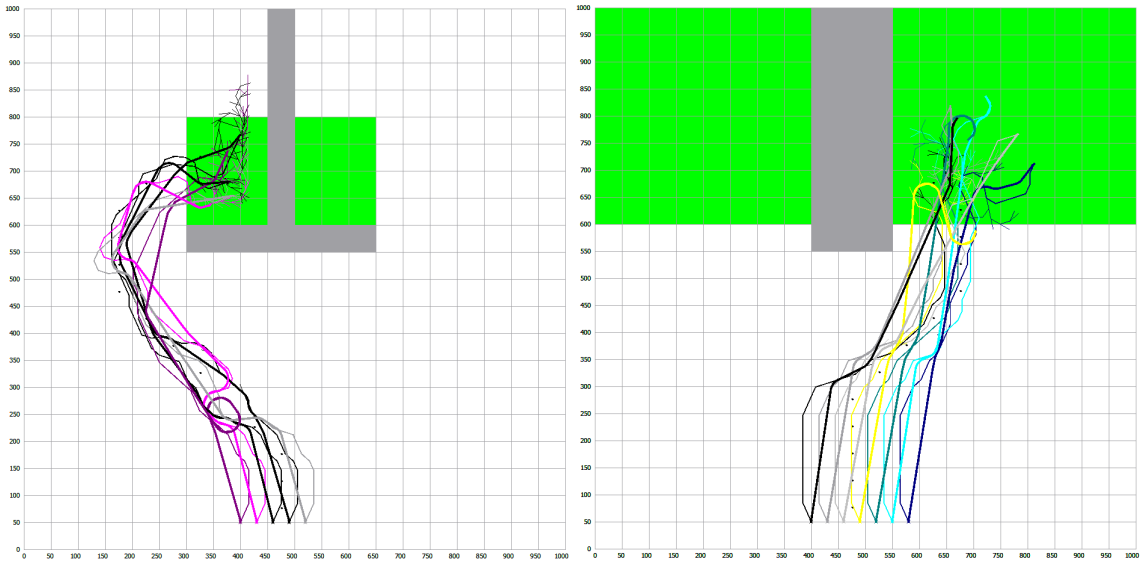

Figure 10.1: Maps with only one covered Area of Interest

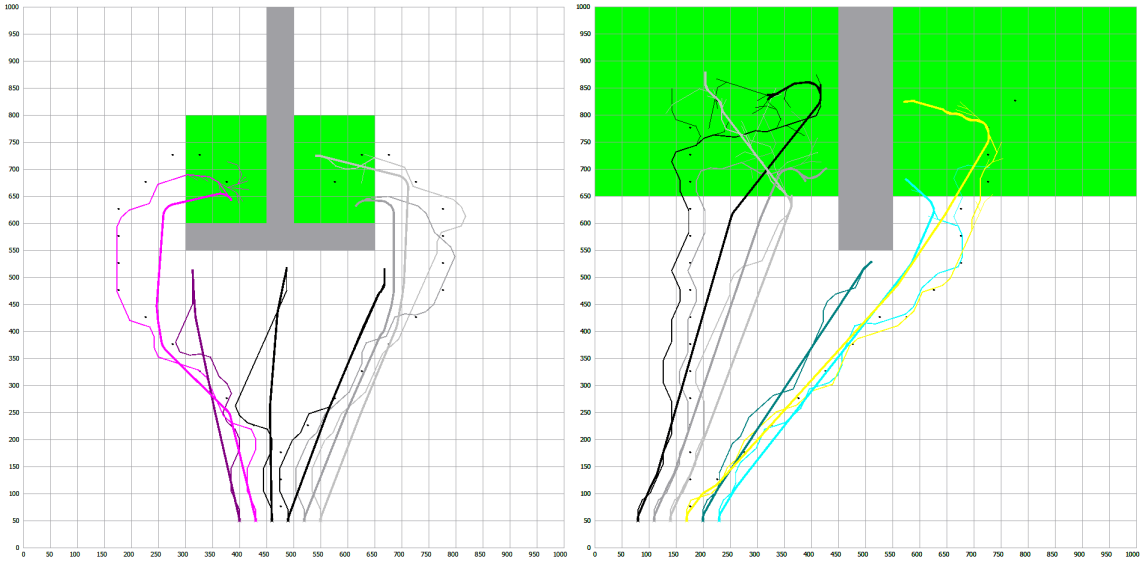

Figure 10.2: Maps with successful chaining behaviour

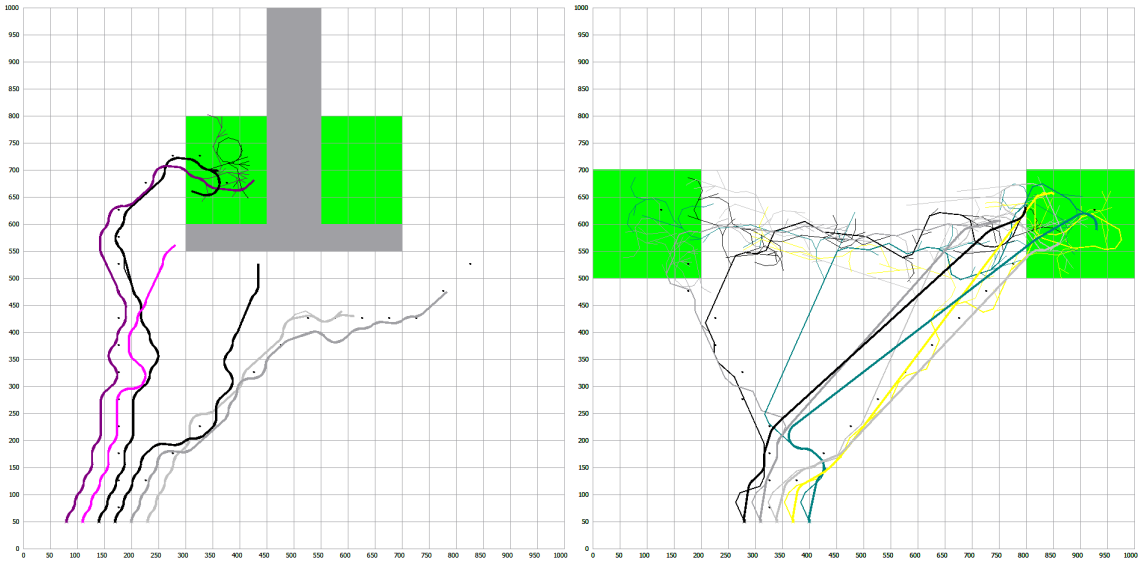

Figure 10.3: Maps with unsuccessful chaining behaviour

tree T which connects middles of all AoIs. When sum of all edges in this tree d_{total} is bigger than $d_{max} = (number\ of\ uavs - 1) \cdot maximal\ distance\ between\ neighbouring\ uavs$, which is maximal length of chain created by UAVs, some AoI and branch leading to its middle will be excluded. This results in shortening the value d_{total}. This process will be repeated while d_{total} will be bigger than maximal d_{max}. When $d_{total} < d_{max}$, we obtain set of AoIs which can be covered by swarm of UAVs. In the next step, UAVs will be split to multiple groups, one group for each AoI. Then the guiding paths will be planned for each groups to reach corresponding branches of T. Then the RRT-Path algorithm will take place. The final step will be optimization by Dubins curves, described in this thesis.

CHAPTER
ELEVEN

V-REP SIMULATIONS

V-REP is acronym for Virtual robot experimentation platform, a simulator developed by Coppelia Robotics, providing an advanced environment for testing and simulations of robots of all types. The V-REP environment is free and open-souce for educational purposes and also has commercial licence. The environment takes in account certain physical laws like gravity, inertia or friction, which enables to truthfully verify applicability for deployment of UAVs in the real world. V-REP has many build-in models, but user can also create his own robot. V-REP enables to control robots over API and has API clients for C, C++, Python, Java, Lua, Matlab, Octave and Urbi.

11.1 UAV control and path simulation

Python is convenient for fast prototyping and has native functions for easy JSON parsing, which made it good choice for simulations of generated trajectories in V-REP.

UAVs in V-REP can be controlled over remote API only by changing location of their target. Then UAV tries to reach the location of its target. Unfortunately, UAVs only follow location, with speed proportional to distance. UAVs do not try to reach target and simultaneously to have zero speed when reaching their target, which causes overshoot. This fact leads to another disadvantage of UAV controller. When keeping target in same distance and direction from UAV, the UAV increases its speed, which causes overshoot when target changes its direction to UAV. These overshoots were many times bigger than size of UAVs, so they could not be ignored and had to be fixed.

During first, naive implementation, position of next state was set as target position for UAV, but due to overshoot and large distances between states UAVs failed to follow the trajectory.

Another implementation linear interpolated trajectory between UAV and its next state position and calculated target placed in line between UAV and next state position, but in constant distance to UAV.

So the calculation was defined as follows

$$\mathbf{X}\left(k+1\right)_{target} = \mathbf{X}\left(k\right)_{UAV} + \frac{\left(\mathbf{X}\left(k\right)_{ns} - \mathbf{X}\left(k\right)_{UAV}\right)}{\|\mathbf{X}\left(k\right)_{ns} - \mathbf{X}\left(k\right)_{UAV}\|} \cdot const$$

where $\mathbf{X}\left(k\right)_{UAV}$ is UAV position in k-th iteration of simulation, $\mathbf{X}\left(k\right)_{ns}$ is position of next state in planned path in k-th iteration, $\mathbf{X}\left(k+1\right)_{target}$ is position of UAV target in $k+1$-th iteration

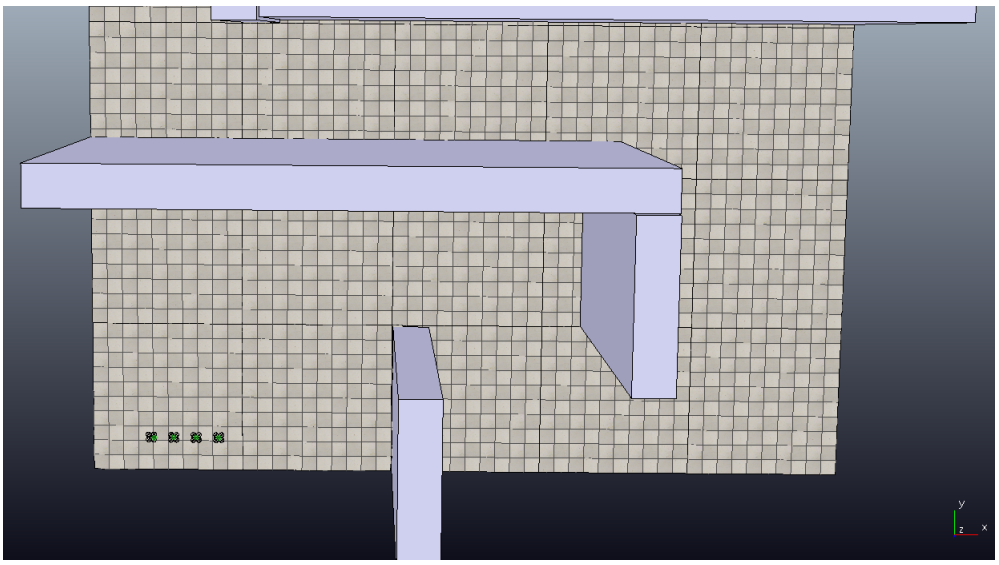

Figure 11.1: Map with UAV overshoot

and *const* is constant experimentally tuned, so the UAV does not move too fast nor too slow. Too fast movements cause overshoot and too slow movements cause the simulation to run for needlessly long time.

But a mentioned earlier, even this approach did not go well. In long passages, where trajectory did not turn, UAVs increased their velocity and inertia, which made them harder to turn. The problem of overshooting is shown in figures 11.1 and 11.2. Overshoot is on the end of long passage in map 11.1. Red and violet balls represent positions of next states and green balls represent UAV targets. In the first image, we can see UAVs leaving the narrow passage. As you can see in second and third image, positions of next state are still, but because of constant distance of target and UAV, the target is dragged by UAVs inertia.

This has been fixed by not updating the position of target when distance between UAV and next state is bigger than in previous iteration and the position of next state is still the same, so the equation describing target position is

$$\mathbf{X}(k+1)_{target} = \begin{cases} \mathbf{X}(k)_{UAV} + \frac{(\mathbf{X}(k)_{ns} - \mathbf{X}(k)_{UAV})}{\|\mathbf{X}(k)_{ns} - \mathbf{X}(k)_{UAV}\|} \cdot const \\ if \, \|\mathbf{X}(k)_{ns} - \mathbf{X}(k)_{UAV}\| < \|\mathbf{X}(k-1)_{ns} - \mathbf{X}(k-1)_{UAV}\| \\ \wedge \mathbf{X}(k)_{ns} = \mathbf{X}(k-1)_{ns} \\ \mathbf{X}(k)_{target} \\ else \end{cases}$$

. This prevents target from dragging by UAV with big inertia.

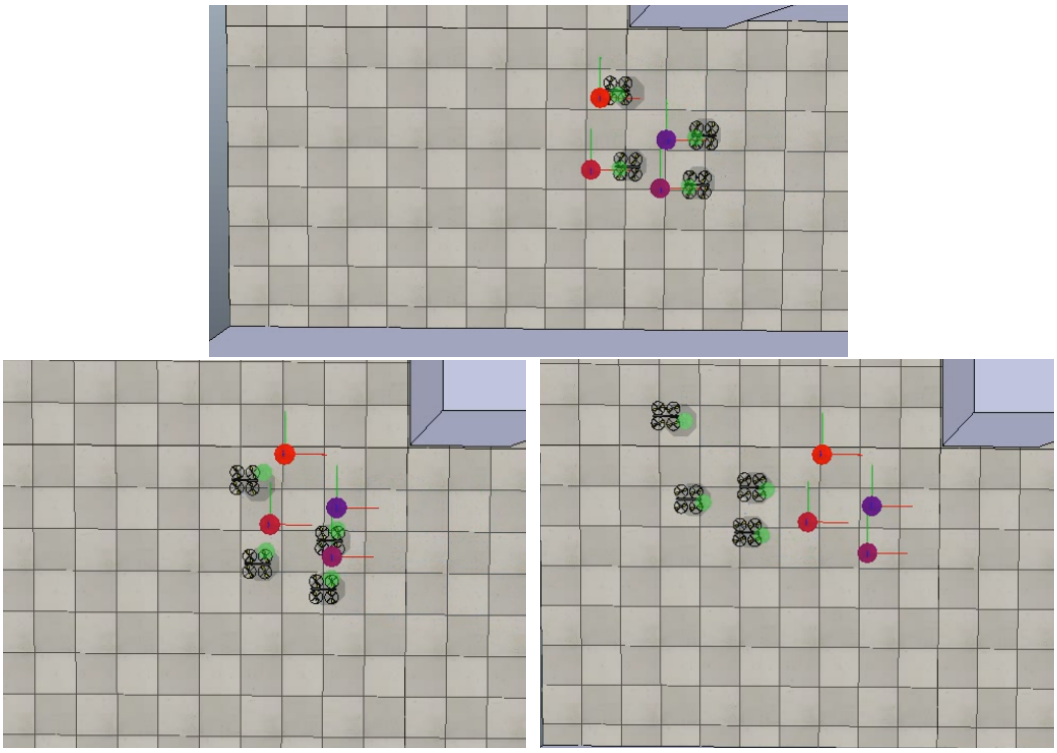

Figure 11.2: UAV overshoot

Here can be seen 3 iterations. Next state is changed during

CHAPTER
TWELVE

IMPLEMENTATION

This part will cover implementation of algorithm, which was used for simulations. Whole codebase in C++ can be found at this github repository. Next to the C++ program, I also created some CLI scripts in PHP, for drawing map and paths from the JSON representation, batch running of Dubins curves optimization and other useful stuff. These can be seen at this github repository. V-REP simulations were made by communicating with V-REP through remote API, the client is written in Python and can be seen here.

12.1 External libraries

Some external libraries are used in the implementation. Every used library is mentioned here. Boost libraries are used for smart pointers, libraries for Dubins curves are from Master Thesis by Petr Váňa [6]. Generating of JSON from C++ object is done via Json Spirit library. Another external library is V-Collide from The University of North Carolina at Chapel Hill.

Because V-Collide sources were written in 1997 and because I used C++11 compiler to compile my source codes, I had to rewrite part of this library for compatibility and to make public API easier to use. Modifications can be seen in this github repository.

Last used external library is QT, which was used to create platform independent GUI.

12.2 Code structure and services

Here is shown brief UML scheme demonstrating dependency diagram of codebase. To keep diagram simple, only services are displayed, other classes, which are not services, were left out for readability. Diagram was generated using software StarUML

Core class holds core of whole Application and has all other classes as dependencies, as is shown in image 12.1.

As mentioned in chapter 2, Configuration is DTO for all configuration variables, but to keep reasonable amount of classes, Configuration is also service, which delegates all configuration changes from GUI to Core class. Configuration and GuiDrawer implementation LoggerInterface are the only connections between Core and GUI.

State factory creates State classes according to Factory pattern. State class represents state in RRT-Path algorithm. State has coordinates and rotations for all UAVs. Persister persists found path to JSON using Json Spirit library. PathHandler serves as utils class for manipulations with

Figure 12.1: Dependency diagram

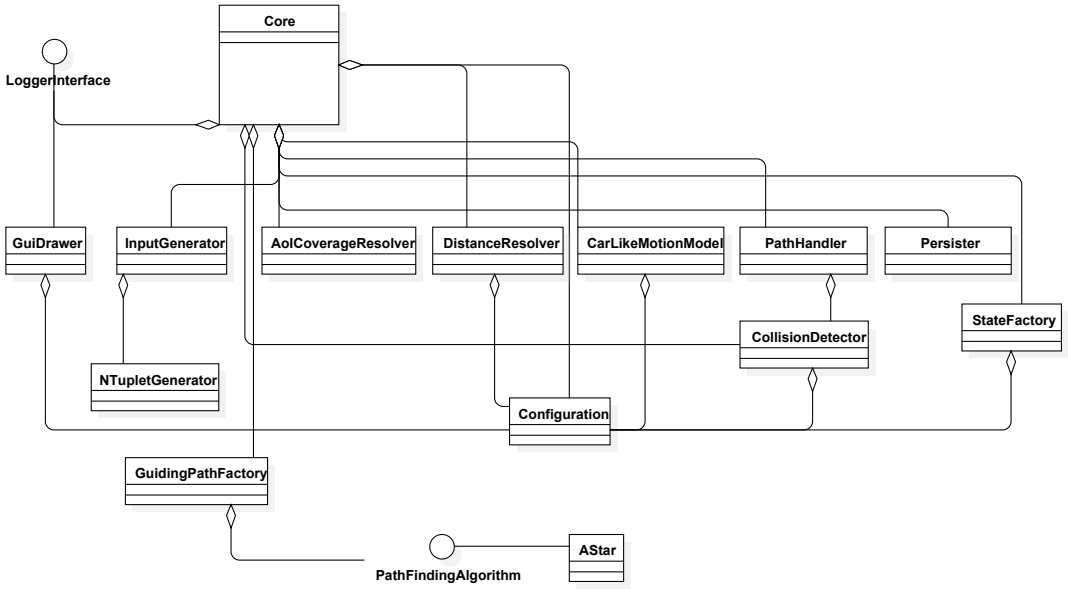

path (vector of State classes). CarLikeMotionModel holds motion model algorithm. InputGenerator is used to generate inputs to motion model. NTupletGenerator only generates variation with repeating for given input. DistanceResolver counts distances between two states and distance of path. AoICoverageResolver determines cost function for states,where all UAVs are in AoIs. GuidingPathFactory is wrapper for PathFindingAlgorithm interface and is used by Core to find guiding path. Implementation of PathFindingAlgorithm is AStart class.

12.3 Utility scripts

All graphs in experiments with re-sampling and Dubins optimization were generated with usage of PHP scripts. Script runDubinsOptimization.php runs sequentially resampling with given frequencies multiple times. This script can be run many times at once with different configuration, which brings advantage of parallel run without need to deals with threads. Script processDubinsOptimizatinData.php merges all CSV result files to one big matrix, with number of rows equal to maximal number of iterations and number of columns equal number of runs of the optimization. For example, as seen in experiment 13.2.1 for frequency 1 Hz it is matrix with size 2095x100. This can be loaded directly to matlab so the graph can be generated. Script drawPaths.php generates map to png image. E. g. map generated by this script can be seen in 13.4.

CHAPTER
THIRTEEN

EXPERIMENTS

13.1 RRT-Path

In this experiment, a path in a map shown in the figure 13.1, is searched by using the RRT-Path algorithm. As we can see, the map is quite complex and has many obstacles. UAVs start in the lower left corner. In this figure, we can also see the path found by RRT-Path algorithm. The algorithm follows the guiding path quite precisely, and whole searching tree for each UAV looks like one long branch. Only the AoI is covered by branches of searching trees. The algorithm is run 1000 times. The algorithm found path to AoI in every run. The results can be seen in the figures 13.2 and 13.3, where can be seen mean value and standard deviation in each iteration of all 1000 runs. In the graph 13.3 we can see total distance between current position of UAVs and their final position above AoI. As we can see, in the beginning, the UAVs are very distant from AoI, but they get closer to goal and try to minimize the distance. The increase of distance to goal corresponds with obstacles avoidance. The graph 13.2, describes distance to nearest neighbour. This experiment has been run with 3 UAVs. In every iteration of the algorithm, each UAV has some nearest neighbour. Distances between the UAV and its nearest neighbour is shown in the graph. This information is important for the relative localization. The minimal and maximal distance are 24 and 180 map units, in this experiment. During the whole path, UAVs fly really close to each other. But in the end, they fly away from each other, because they can cover bigger part of AoI when they have bigger distance between each other.

13.2 Influence of re-sampling on Dubins curves optimization

To demonstrate the optimization, few maps were selected to be used in re-sampling and optimization experiments. The RRT-Path algorithm found trajectories for UAVs. These trajectories were re-sampled and optimized 100 times to obtain relevant results because of using random numbers during the optimization and avoiding getting stuck in local optima.

Due to time and memory consumption, each optimization is stopped after 200 iterations where optimization did not shorten the path or when speed of path shortening was slower than 5% of original path length per 1000 iterations.

The algorithm also stops when consumed memory exceeds 1900 MB. This is right before shutting of program by operating system, because 32bit processes are not allowed to use more than 2 GB of RAM. This feature was implemented using an ugly platform-dependent hack.

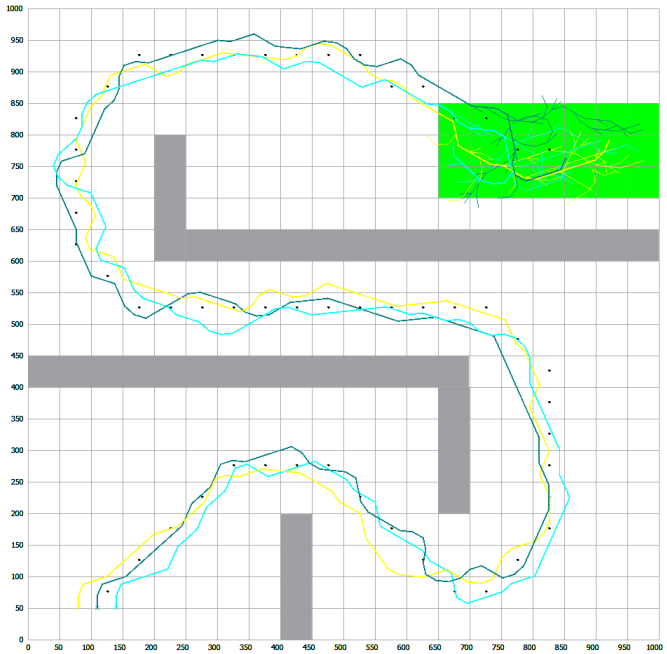

Figure 13.1: Map used for experiment

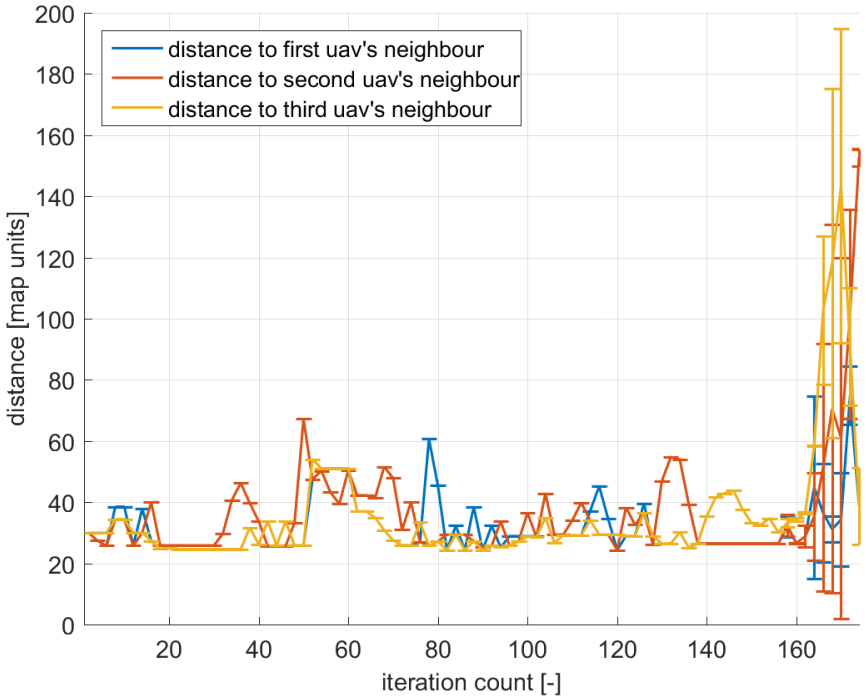

Figure 13.2: Distances between nearest UAVs in swarm and distance to AoI

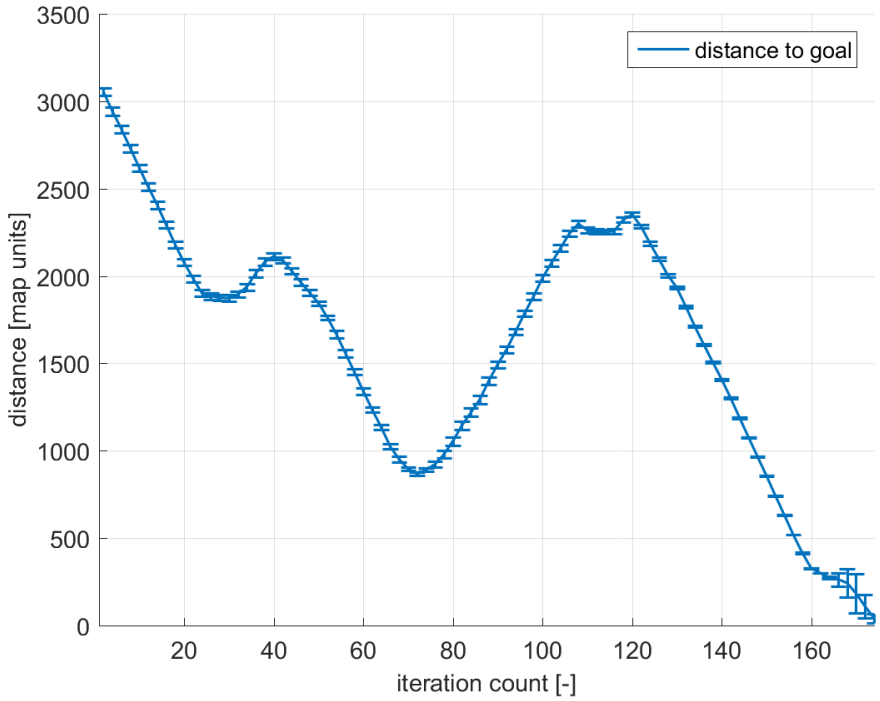

Figure 13.3: Distance between UAVs ans AoI

In next sections, maps with obstacles, AoIs and trajectories will be shown. Obstacles are grey rectangles, AoI is green rectangle and each UAV has trajectory marked with different colour. For measuring of influence of re-sampling of path to Dubins curves optimization, following frequencies were selected: 1 Hz (initial frequency used in RRT-Path algorithm), 2 Hz, 4 Hz, 6 Hz, 8 Hz, 10 Hz, 12 Hz, 14 Hz, 16 Hz, 18 Hz, 20 Hz.

13.2.1 First experiment

The map with trajectories found by the RRT-Path algorithm can be seen in 13.4.

The best result of Dubins curves optimization (re-sampling of 20Hz) is shown in 13.5. As we can see, trajectories are much shorter than trajectories before optimization in 13.4. On the beginning of trajectories, in the left upper corner of picture, we can see much smoother curves than before optimization. This is due to re-sampling to frequency 20Hz, which smooths trajectories.

In real flight, it is undesirable to have trajectories tight to obstacles, so obstacles are amplified before optimization. This can be seen in 13.5 where UAVs keep certain distance from the obstacles.

Following table shows average total, minimal and maximal distance of all trajectories from 100 optimizations after the re-sampling and optimization.

The results are also shown in graph 13.6. On the graph we can see that initial frequency 1 Hz has worst results and the frequency 20 Hz has best results. We can also see that in frequency 14 Hz and higher, all 100 iterations had same results, the minimum, maximum and mean value are the same. But the second best frequency in terms of minimal, maximal and mean value is 6 Hz and even the worst optimization in 6 Hz has smaller total distance than 8 to 18 Hz.

Figure 13.4: Path before Dubins curves optimization

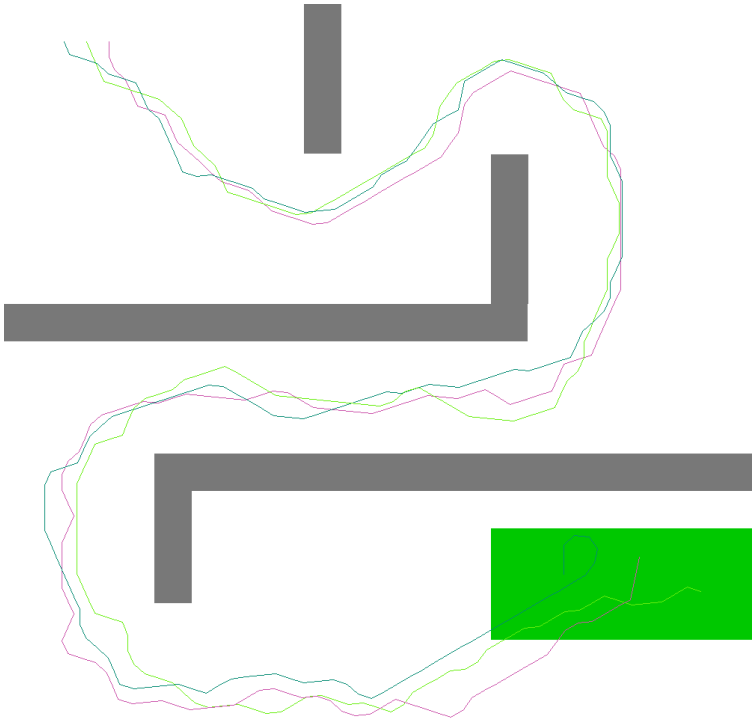

Figure 13.5: Path after Dubins curves optimization

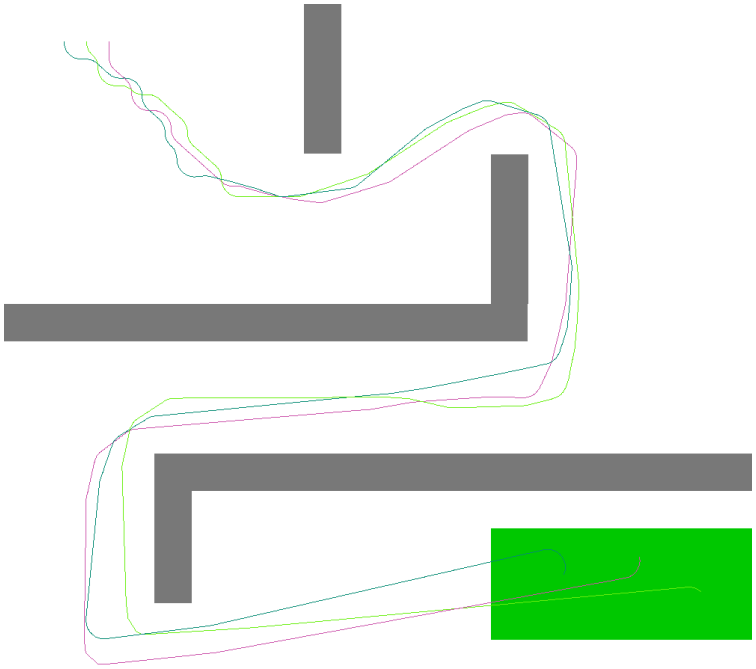

Table 13.1: Re-sampling and optimization results

Frequency [Hz]	Minimal distance [m]	Maximal distance [m]	Average distance [m]
1	8582.18	8849.7	8721.2904
2	8311.65	8548.81	8430.23
4	8366.88	8393.09	8379.985
6	8248.9	8275.7	8262.3
8	8249.88	8378.51	8314.195
10	8286.22	8472.2	8379.21
12	8302.51	8309.2	8307.6613
14	8303.18	8303.18	8303.18
16	8363.92	8363.92	8363.92
18	8510.32	8510.32	8510.32
20	8194.22	8194.22	8194.22

Figure 13.6: Re-sampling and optimization results graph

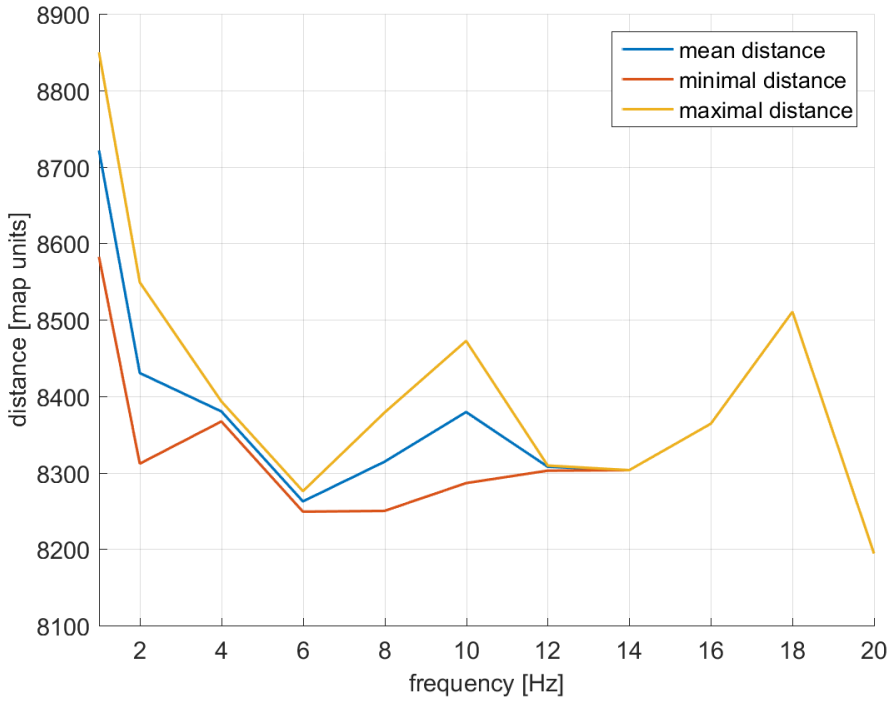

Figure 13.7: Time course of optimization for 2 Hz, 4 Hz, 6 Hz

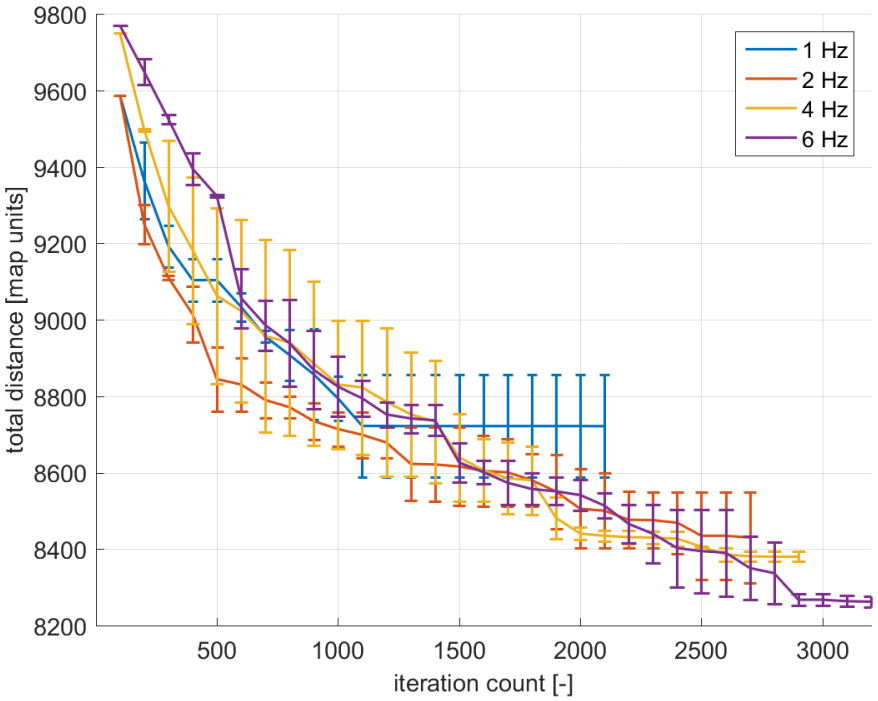

Depending on re-sampling frequency, the courses of optimization are also different.

In 13.7, 13.8 and 13.9 we can see mean values and standard deviations for different frequencies, divided into three graphs for better readability. The vertical lines are error bars, they show standard deviation during the optimization. Because the error bars would be too dense if they were shown for each iteration, only every 100th iteration is shown on graphs. For comparison, on each graph is shown also frequency 1 Hz, the initial frequency before re-sampling. As we can see, frequencies 14, 16, 18 and 20 Hz have almost zero standard deviation and converge to lower value than initial frequency. In frequency 10 Hz can be seen high standard deviation. That means the optimization got stuck in local optimum and was not able to shorten any path for many iterations.

13.2.2 Second experiment

The best result of Dubins curves optimization (re-sampling of 4Hz) is shown in 13.11. As we can see, trajectories are much shorter than trajectories before optimization in 13.10, as in experiment 1, but curves in the upper part of figure still were not optimized. This was caused by optimization algorithm getting stuck in local optimum. The algorithm tried to optimize other parts and ended due to stopping conditions mentioned above. Light grey colour represents obstacle amplification.

The results are shown in graph 13.12. On the graph can be seen interesting results. Contrary to the graph from experiment 1 13.6, all frequencies have same minimal distance, maximal distance and mean distance. This shows us interesting fact. For same frequency, all 100 runs got stuck in same local optimum, but every frequency has different local optimum where the algorithm can stuck. Trajectory in this experiment is much smaller, which leads to zero standard

Figure 13.8: Time course of optimization for 8 Hz, 10 Hz, 12 Hz

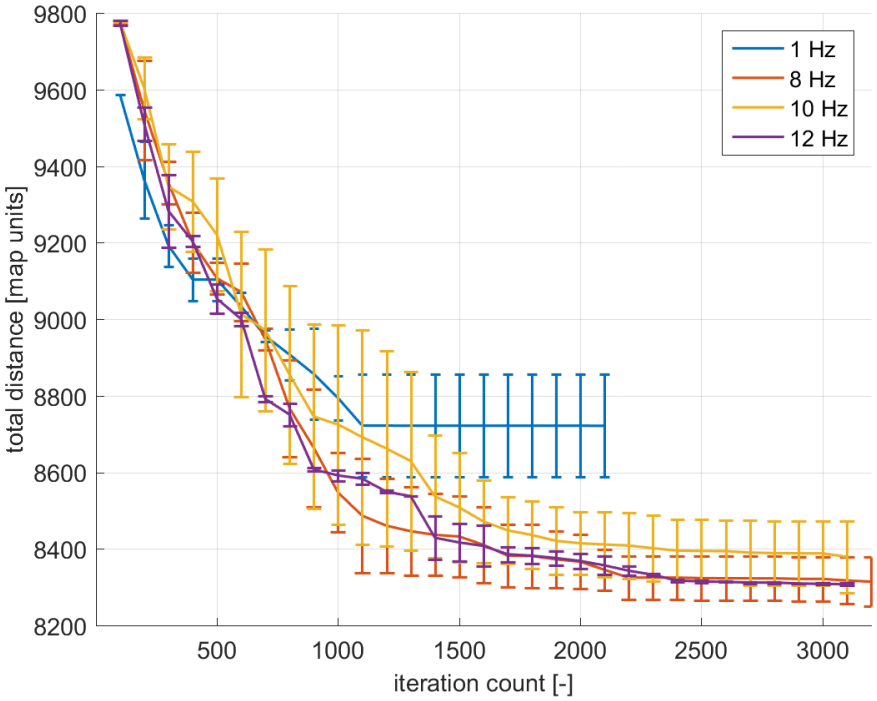

Figure 13.9: Time course of optimization for 14 Hz, 16 Hz, 18 Hz, 20 Hz

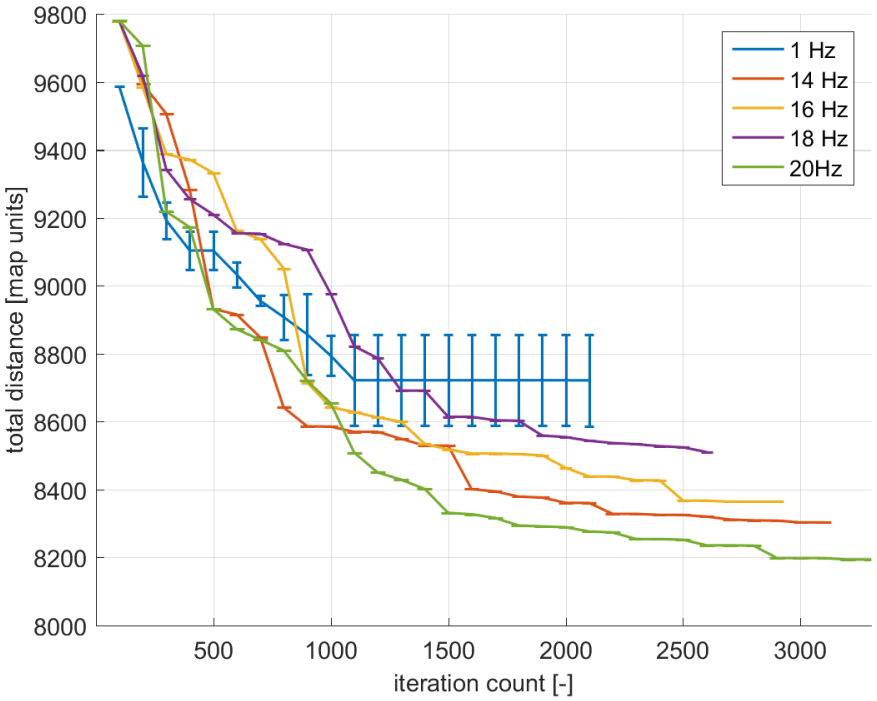

Figure 13.10: Path before Dubins curves optimization

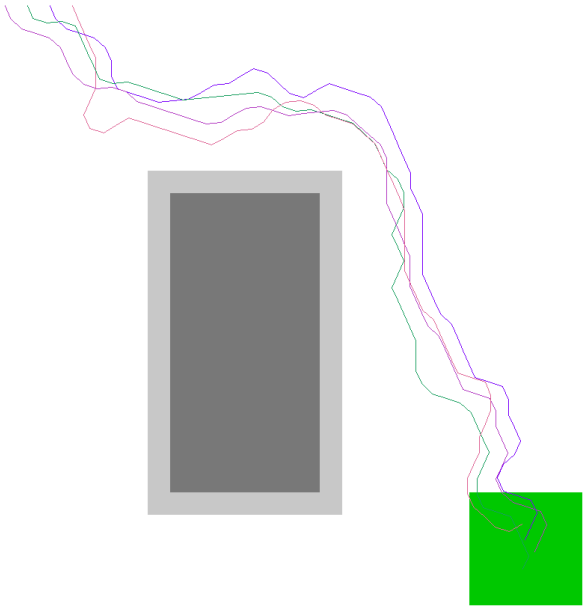

Figure 13.11: Path after Dubins curves optimization

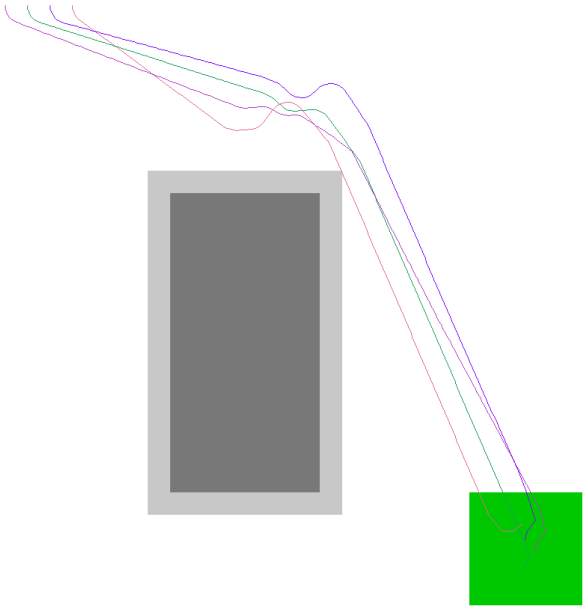

Figure 13.12: Re-sampling and optimization results graph

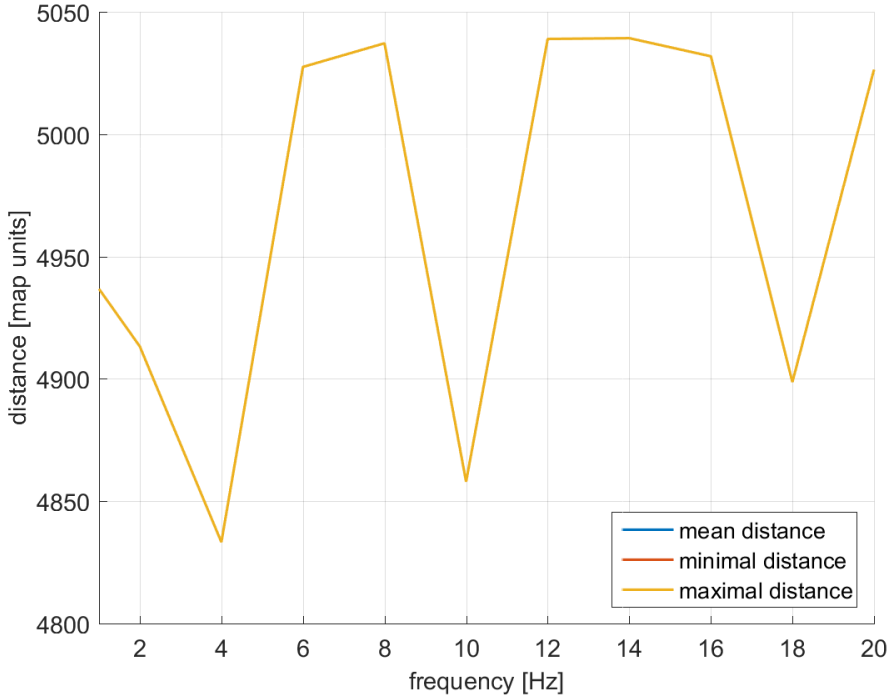

deviation and difference between minimal and maximal distance between optimization results in one frequency. The difference between maximal and minimal results is bigger when optimizing longer and more complicated trajectory. As we can also see from graphs, we can not predict optimal re-sampling frequency from trajectory.

Depending on re-sampling frequency, the courses of optimization are also different.

In 13.13, 13.14 and 13.15 we can see mean values and standard deviations for different frequencies, divided into three graphs for better readability. The vertical lines are error bars, they show standard deviation during the optimization. Because the error bars would be too dense if they were shown for each iteration, only every 10th iteration is shown on graphs. For comparison, on each graph is shown also frequency 1 Hz, the initial frequency before re-sampling. As we can see, in comparison to experiment 1, standard deviations are zero, so the optimization algorithm exhibits deterministic behaviour even if this optimization method is stochastic.

Figure 13.13: Time course of optimization for 2 Hz, 4 Hz, 6 Hz

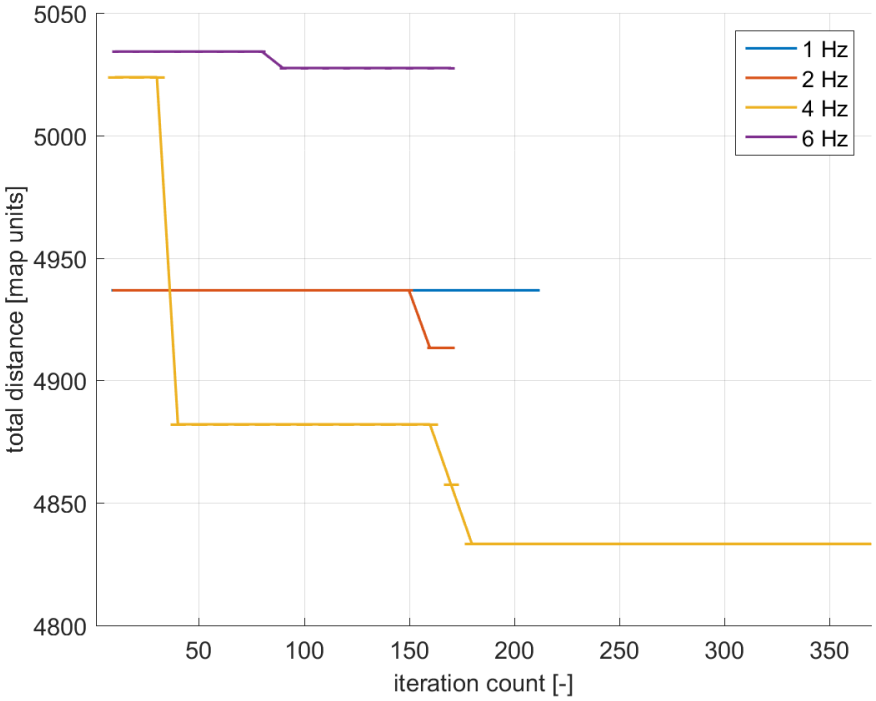

Figure 13.14: Time course of optimization for 8 Hz, 10 Hz, 12 Hz

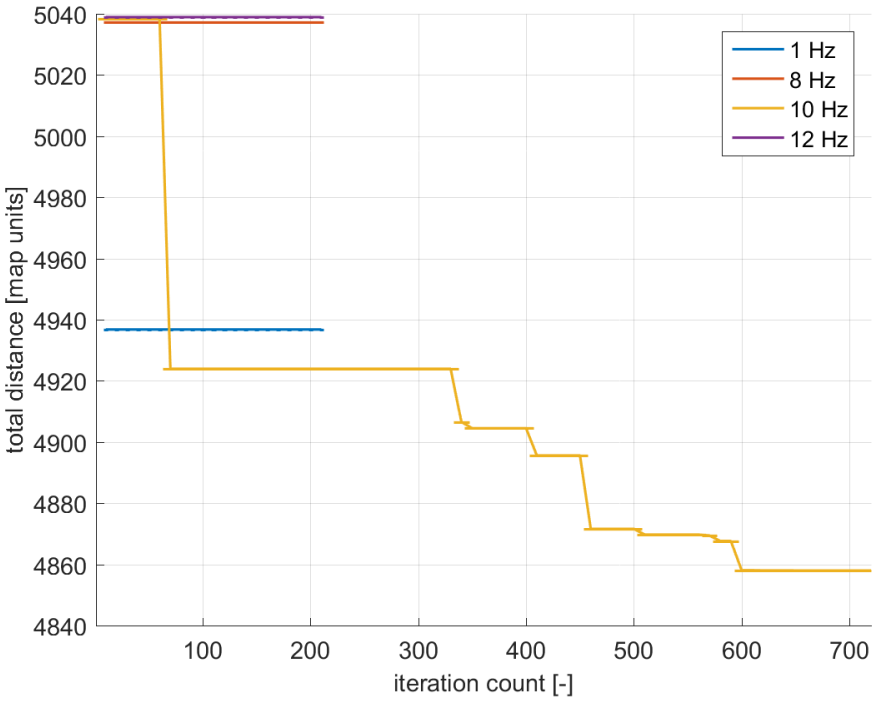

Figure 13.15: Time course of optimization for 14 Hz, 16 Hz, 18 Hz, 20 Hz

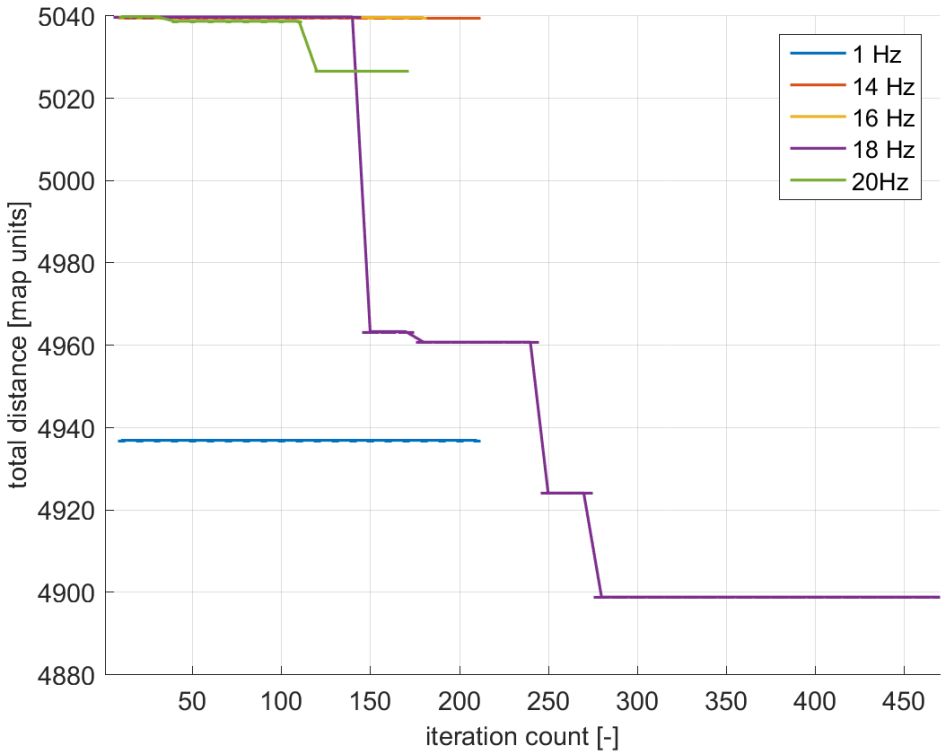

BIBLIOGRAPHY

[1] Lester Eli Dubins. On curves of minimal length with a constraint on average curvature, and with prescribed initial and terminal positions and tangents. *American Journal of Mathematics*, 79(3):497–516, July 1957. URL http://www.jstor.org/stable/2372560?origin=crossref&seq=1#page_scan_tab_contents.

[2] Jan Faigl, Tomáš Krajník, Jan Chudoba, and Martin Saska. Low-cost embedded system for relative localization in robotic swarms. *Robotics and Automation (ICRA), 2013 IEEE International Conference on*, pages 993 – 998, May 2013.

[3] Steven M. LaValle. Rapidly-exploring random trees: A new tool for path planning. Technical report, Department of Computer Science, Iowa State University, 1998. URL http://msl.cs.uiuc.edu/~lavalle/papers/Lav98c.pdf.

[4] Steven M. LaValle. *Planning Algoritms*. Cambridge University Press, 2006. URL http://planning.cs.uiuc.edu/.

[5] Matěj Petrlík. Planning of swarm deployment for autonomous surveillance. Bachelor's thesis, Czech technical university in Prague Faculty of Electrical Engineering Department of Cybernetics, 2015.

[6] Petr Váňa. Path planning for non-holonomic vehicle in surveillance missions. Master's thesis, Czech Technical University in Prague, 2015. URL https://dspace.cvut.cz/bitstream/handle/10467/61814/F3-DP-2015-Vana-Petr-thesis.pdf.

[7] Vojtěch Vonásek. *A guided approach to sampling-based motion planning*. PhD thesis, Czech Technical University in Prague Faculty of electrical engineering Department of cybernetics, August 2015.

CHAPTER
FOURTEEN

CONCLUSION

In this thesis, I described and implemented and experimentally verified usage of the motion planning RRT-Path algorithm.The algorithm contains relative localization and motion model, which makes it usable for motion planning of real swarms.